Available online at www.sciencedirect.com
ScienceDirect
Tetrahedron
Tetrahedron 62 (2006) 10821–10828

A computational study of halomethyllithium carbenoid mixed aggregates with lithium halides and lithium methoxide

Lawrence M. Pratt,[a,*] Shayla Merry,[a] Son Chi Nguyen,[b] Phung Quan[b] and B. T. Thanh[b]

[a]*Department of Chemistry, Fisk University, 1000 17th Avenue North, Nashville, TN 37209, United States*
[b]*Vietnam National University, University of Natural Sciences, 227 Duong Nguyen Van Cu, District 5, Ho Chi Minh City, Vietnam*

Received 16 July 2006; revised 16 August 2006; accepted 29 August 2006
Available online 20 September 2006

Abstract—Density functional theory calculations were used to examine the formation of lithium halide and lithium alkoxide mixed aggregates with halomethyllithium carbenoids. These mixed aggregates may be the important intermediates in carbenoid reactions where lithium halides are formed as byproducts, or when the mixture has been exposed to small amounts of air. The calculations showed that in the gas phase and in THF solution, mixed dimers, trimers, and tetramers may coexist with free lithium carbenoids, depending on the lithium salt. The calculations also indicated that mixed aggregates may influence the activation free energies of cyclopropanation reactions of lithium carbenoids.

1. Introduction

Lithium carbenoids are used extensively in organic synthesis. In addition to cyclopropanation reactions with alkenes, carbenoids undergo a variety of single bond insertion reactions, including both C–H and C–heteroatom insertions. The instability and reactivity of lithium carbenoids makes them difficult to study by conventional experimental methods, although low temperature ^{13}C NMR spectroscopy has been used for structure determination of a few of the more stable haloalkyllithium carbenoids.[1,2] Those investigations proved the carbene-like character of the halomethyllithium species from the lithium–carbon spin coupling constants, but provided no information on the aggregation behavior of lithium carbenoids. To date little is known about the detailed reaction mechanisms of these compounds, and several research groups have turned to computational studies to investigate the structure and reactions of these species in more detail. Cyclopropanation reactions have been the subject of several theoretical investigations of monomeric lithium and zinc carbenoids in the gas phase.[3–5]

Nearly all organolithium compounds can exist as aggregates, and lithium carbenoids are no exception. A previous computational study showed that halomethyllithium carbenoids dimerize in the gas phase and sometimes in ethereal solvents.[6] Small changes in the structure of lithium compounds or in solvation can cause significant changes in the aggregation behavior. Mixed aggregates between two different lithium compounds are also quite common and can have significant effects on the product distribution. This was illustrated by several studies on lithium dialkylamide mixed aggregates and their effect on the stereochemistry of ketone enolization.[7–12]

A clear picture of the reactions of lithium carbenoids is beginning to emerge, and will almost certainly include homo- and mixed aggregates. Nakamura and co-workers showed that monomeric lithium and zinc carbenoids can react with alkenes either in a concerted or stepwise manner.[3] Our own work, currently in progress, suggests that the concerted mechanism is also operative in the lithium carbenoid dimer. The monomer and homo-dimer are likely reactive species at the beginning of lithium carbenoid reactions before much lithium halide byproduct has been formed. We hypothesize that the lithium halide byproduct will form mixed aggregates with the halomethyllithium carbenoids, similar to those that have recently been reported with lithium dialkylamides.[13] Likewise, exposure of the reaction mixture, or the alkyllithium used to generate the carbenoid, to small amounts of air will result in the formation of lithium alkoxides. Of course, either of those compounds can be intentionally added to the reaction mixture to take advantage of any favorable reactions of mixed aggregates, and addition of LiCl to reaction mixtures of lithium compounds is quite common. In this paper we use computational methods to elucidate the structures and solvation states of lithium carbenoid mixed aggregates with lithium halides and lithium methoxide. In addition, we investigate whether mixed aggregates significantly alter the activation free energy of cyclopropane formation between chloromethyllithium and ethylene. The

Keywords: Lithium carbenoids; Mixed aggregates; Molecular modeling; DFT.
* Corresponding author. Tel.: +1 615 3298559; e-mail: lpratt@fisk.edu

0040–4020/$ - see front matter © 2006 Elsevier Ltd. All rights reserved.
doi:10.1016/j.tet.2006.08.104

significance of this is that lithium carbenoids may undergo several types of insertion reactions, or non-insertion reactions like the FBW rearrangement of 1-halovinyllithium carbenoids. The competition between the different types of reactions is likely influenced by mixed aggregates.

2. Computational methods

All calculations were performed using the *Gaussian 98* or *Gaussian 03* programs.[14] The reported gas phase and solution energies include the electronic and nuclear repulsion energy (E_{en}), thermal corrections to the free energy (including ZPE) at 200 and 298 K, and where applicable, solvation terms. Due to the possibility of several possible conformations of similar energy, it was sometimes necessary to optimize two or more conformations of the same structure and the lowest energy conformer was used in subsequent calculations.

The solvation free energy change of the gas phase organolithium molecule $(RLi)_n$ due to microsolvation by m explicit ethereal solvent ligands E (in this case, THF) is calculated by considering the process

$$(RLi)_n + mE \rightarrow (RLi)_n \cdot mE. \quad (1)$$

The microsolvation model assumes that the free energy change accompanying this reaction adequately represents the solvation free energy ΔG^{o}_{solv}, of the solute $(RLi)_n$ in the solvent E, so that

$$G^{o}_{T}(\text{solute}) = G^{o}_{T}(\text{gas}) + \Delta G^{o}_{solv} \quad (2)$$

In other words, the free energy of a 'supermolecule' $(RLi)_n \cdot mE$ relative to that of m solvent molecules is assumed to yield a good approximation to the free energy of the solvated molecule $(RLi)_n$ in the condensed phase. The gas phase free energies at temperature T of the relevant species are obtained computationally as

$$G^{o}_{T}(\text{gas}) = E_{en} + \Delta G^{o}_{T}, \quad (3)$$

where the terms on the right hand side as well as the procedure used for calculating them are described below. The geometry of each molecule or transition structure was first optimized using the B3LYP hybrid density functional method[15,16] with the MIDIX basis set,[17] and that basis set was also used for frequency calculations and to determine the ZPE's and thermal corrections to the free energies. A further refinement of the geometry and electronic energy was done at the B3LYP/6-31+G(d)[18,19] level of theory, as diffuse functions are needed for molecules that have substantial carbanion character. Basis set superposition errors (BSSE) were corrected by counterpoise corrections for all homo- and mixed aggregates, defining the fragments in each aggregate as the lithium carbenoid or lithium halide monomer units. When calculating the energies of mixed aggregate formation, each aggregated species was counterpoise corrected at the B3LYP/6-31+G(d) level, including the lithium carbenoid and lithium halide dimers. Thus we have:

E_{en}=the electronic plus nuclear repulsion energy of the equilibrium geometry, using B3LYP/6-31+G(d).

E^{vib}_{0}=unscaled B3LYP/MIDIX vibrational zero point energy.

ΔG^{o}_{T}=B3LYP/MIDIX thermal corrections to the free energy for a standard state of 1 atm and specified temperature from the masses. This includes contributions from translational, rotational, and vibrational degrees of freedom, as well as the zero point energy.

Calculations of the free energy changes for the 'reactions' (dimerizations, tetramerizations, etc.) are straightforward using the G^{o}_{T}(gas) terms defined in Eq. 3.

Density functional theory is not always reliable for transition structure calculations, so a slightly different approach was used to determine activation free energies. The geometry was optimized and the thermal corrections to the free energies were obtained at the Hartree–Fock/6-31+G(d) level. The geometries were then re-optimized at the B3LYP and MP2 levels with the same basis set, and the Hartree–Fock thermal corrections were added to the E_{en} at each level of theory to obtain approximate activation free energies.

The standard state of a solution is taken as 1 mol/L at 298.15 K, and an additional correction to the free energy terms is needed to convert the standard state of an ideal gas (1 atm) to the standard state of the solution. This was incorporated by simply adding the term $RT\ln(RT)$ to each free energy term, where the numerical value of the argument of the logarithm was obtained using the pressure–volume (0.082057 L atm/K/mol) value for the gas constant. This replaces the logarithm argument term PV (24.47 L atm) with RT, corresponding to a concentration of approximately 0.0409 mol/L, and this correction corresponds to the free energy of compressing the gas to a concentration of 1 mol/L. These corrections amount to 1.1120 kcal/mol at 200 K and 1.8943 kcal/mol at 298 K. These correction terms were included in all solution phase reactions below, i.e., calculations where the microsolvation model was used.

Yet another correction is required for proper treatment of the explicit solvent molecules used in microsolvation. The traditional approach is to set the standard state of a pure liquid to be the concentration of the pure liquid itself, which then allows one to drop the concentration of the pure liquid from equilibrium expressions (consider the ionic product of water, for example). However, since we have decided to adopt the standard state of 1 mol/L for all species, the free energy change for the process

$$2RLi \cdot 2THF \rightarrow (RLi \cdot THF)_2 + 2THF \quad (4)$$

is given by Ref. 20

$$\Delta G^{o} = -RT\ln\left\{\left[(RLi \cdot THF)_2\right]/[RLi \cdot 2THF]^2\right\} - 2RT\ln[THF] \quad (5)$$

The molarity of the THF solvent was calculated to be 13.26 at 200 K, and 12.33 at 298 K, from its tabulated density.[21] These corrections amount to −1.0273 and −1.4883 kcal/mol per THF at 200 and 298 K, respectively. Thus, the $-2RT\ln[THF]$ term in Eq. 5 will favor the disolvated monomer by 2.0546 kcal/mol at 200 K.

3. Results and discussion

Because frequency calculations on large systems are often prohibitively expensive, the smaller MIDIX basis set was used to calculate the thermal corrections to the free energies. To be sure that those corrections were reasonable, the geometries of gas phase carbenoid monomers and dimers were optimized with both the MIDIX and 6-31+G(d) basis sets and the thermal corrections calculated, as shown in Table 1. The total thermal correction for the dimerization of the halomethyllithiums is the correction to the dimer free energy minus twice the correction to the monomer, shown in the last column of Table 1. The differences between the MIDIX and 6-31+G(d) results were 0.8 and 0.5 kcal/mol, respectively, for the dimerization of chloro- and bromomethyllithium. We therefore concluded that the use of the smaller basis set for the frequencies is a reasonable approximation for this system.

Table 1. Calculated thermal corrections to the free energy (Hartree) for the dimerization of lithium carbenoids

Carbenoid	Basis set	Monomer	Dimer	$D-2M$
$LiCH_2Cl$	MIDIX	0.000844	0.022119	0.020431
$LiCH_2Cl$	6-31+G(d)	0.000762	0.020666	0.019142
$LiCH_2Br$	MIDIX	−0.000875	0.017992	0.019742
$LiCH_2Br$	6-31+G(d)	−0.000838	0.017277	0.018953

The free energies of mixed aggregate formation were calculated from the free energies of the lithium carbenoid and lithium halide dimers. The lithium halide dimers were used in these calculations based on the experimental result that LiBr is mostly dimeric in THF solution.[22] Lithium methoxide could potentially exist as a dimer or tetramer, and the energy of gas phase and THF solvated tetramer formation was calculated according to Eqs. 6 and 7, respectively. The calculated energies at the counterpoise corrected B3LYP/6-31+G(d) level are shown in Table 2. In both the gas phase and in solution, the tetramer was energetically favored, and that the species was used in the calculation of mixed aggregate energies of formation.

$$2(LiOCH_3)_2 \rightarrow (LiOCH_3)_4 \quad (6)$$

$$2(LiOCH_3)_2 \cdot 2THF \rightarrow (LiOCH_3)_4 \cdot 4THF \quad (7)$$

The mixed aggregates that were investigated include a mixed dimer, two mixed trimers, and four mixed tetramers. The mixed aggregate structures and free energies of formation were first calculated in the gas phase to determine the aggregation behavior in the absence of solvent effects, and then using the microsolvation model with THF ligands. Because basis set superposition errors (BSSE) can be substantial with lithium halides (particularly bromides), all reported free energies were counterpoise corrected, as described in the Section 2. The gas phase free energies of lithium halide mixed aggregate formation were calculated according to Eqs. 8–13, and the corresponding lithium methoxide mixed aggregates by Eqs. 14–19. The optimized gas phase geometries of the chloromethyllithium carbenoids and their mixed aggregates (structures **1**–**9**) are shown in Figure 1, and the analogous lithium methoxide tetramer and mixed aggregates (structures **10**–**17**) are shown in Figure 2. The lithium

Table 2. Calculated free energies of lithium methoxide tetramer formation (kcal/mol)

Phase	Temp (K)	ΔG tetramer formation
Gas	200	−35.8
Gas	298.15	−31.6
THF solution	200	−13.4
THF solution	298.15	−8.11

chloro- and bromocarbenoid mixed aggregates optimized to similar geometries.

$$1/2(LiCH_2X)_2\ (\mathbf{1}) + 1/2(LiX)_2\ (\mathbf{2}) \rightarrow (LiCH_2X)(LiX)\ (\mathbf{3}) \quad (8)$$

$$1/2(LiCH_2X)_2 + (LiX)_2 \rightarrow (LiCH_2X)(LiX)_2\ (\mathbf{4}) \quad (9)$$

$$(LiCH_2X)_2 + 1/2(LiX)_2 \rightarrow (LiCH_2X)_2(LiX)\ (\mathbf{5}) \quad (10)$$

$$(LiCH_2X)_2 + (LiX)_2 \rightarrow (LiCH_2X)_2(LiX)_2 \text{ (two isomers, } \mathbf{6} \text{ and } \mathbf{7}) \quad (11)$$

$$1/2(LiCH_2X)_2 + 3/2(LiX)_2 \rightarrow (LiCH_2X)(LiX)_3\ (\mathbf{8}) \quad (12)$$

$$3/2(LiCH_2X)_2 + 1/2(LiX)_2 \rightarrow (LiCH_2X)_3(LiX)\ (\mathbf{9}) \quad (13)$$

$$1/2(LiCH_2X)_2\ (\mathbf{1}) + 1/4(LiOMe)_4\ (\mathbf{10}) \rightarrow (LiCH_2X)(LiOMe)\ (\mathbf{11}) \quad (14)$$

$$1/2(LiCH_2X)_2\ (\mathbf{1}) + 1/2(LiOMe)_4\ (\mathbf{10}) \rightarrow (LiCH_2X)(LiOMe)_2\ (\mathbf{12}) \quad (15)$$

$$(LiCH_2X)_2\ (\mathbf{1}) + 1/4(LiOMe)_4\ (\mathbf{10}) \rightarrow (LiCH_2X)_2(LiOMe)\ (\mathbf{13}) \quad (16)$$

$$(LiCH_2X)_2 + 1/2(LiOMe)_4 \rightarrow (LiCH_2X)_2(LiOMe)_2 \text{ (two isomers, } \mathbf{14} \text{ and } \mathbf{15}) \quad (17)$$

$$1/2(LiCH_2X)_2 + 3/4(LiOMe)_4 \rightarrow (LiCH_2X)(LiOMe)_3\ (\mathbf{16}) \quad (18)$$

$$3/2(LiCH_2X)_2 + 1/4(LiOMe)_2 \rightarrow (LiCH_2X)_3(LiOMe)\ (\mathbf{17}) \quad (19)$$

The calculated free energies of gas phase mixed dimer and trimer formation are shown in Table 3. For each system, mixed trimer formation is favored over mixed dimer formation, and the formation of both mixed aggregates is weakly temperature dependent, with the higher temperature disfavoring lithium halide mixed aggregate formation. Formation of lithium halide mixed dimers and trimers is more energetically favored than those of lithium methoxide. In the gas phase, steric effects on the chloromethyllithium dimer are negligible, and the driving force toward mixed aggregate formation is likely to be primarily the difference in base strengths of the carbenoid and the lithium salt.

Table 4 shows the calculated free energies for mixed tetramer formation. Two isomeric $(LiCH_2X)_2(LiX)_2$ mixed tetramers optimized to planar ladder (**6**) and distorted tetrahedral (**7**) geometries, with the ladder structure being favored by about 0.5–1 kcal/mol per lithium atom. The analogous lithium methoxide symmetrically mixed tetramers optimized to a ladder (**14**) or bent (**15**) geometry, with the ladder structure

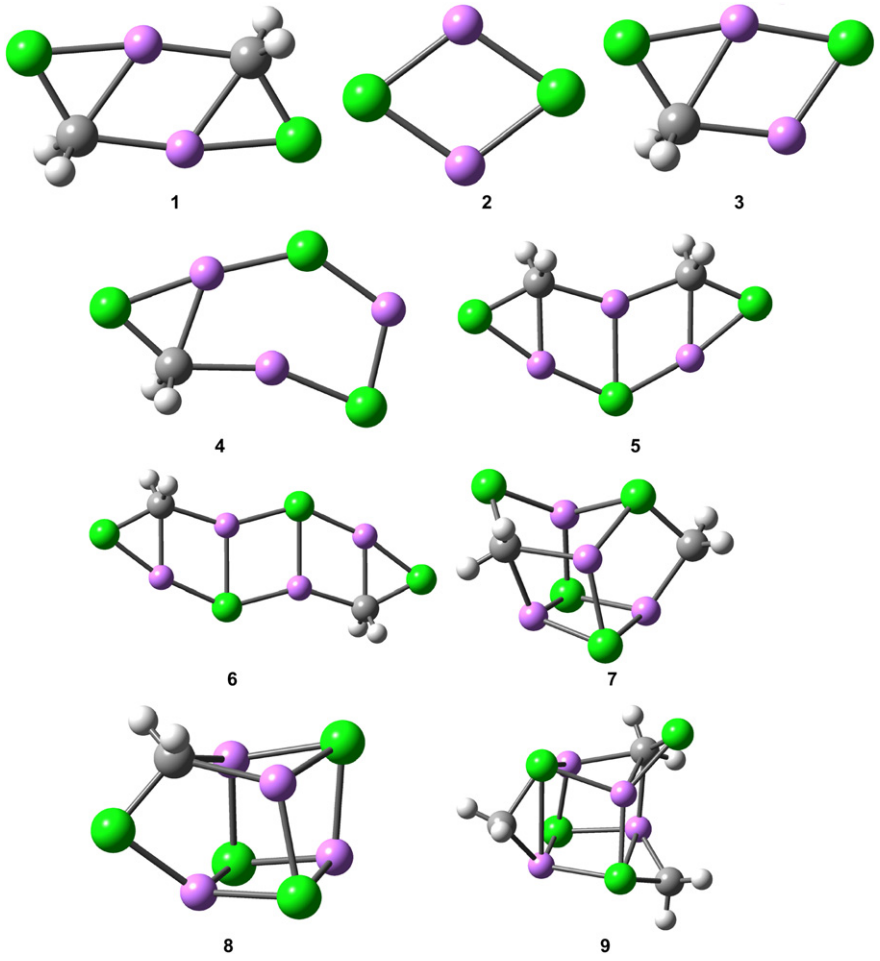

Figure 1. Optimized geometries of gas phase chloromethyllithium, LiCl, and mixed aggregates **1–9**. Gray: carbon; white: hydrogen; violet: lithium; green: chlorine; red: oxygen.

being highly favored over the bent one. The two unsymmetrically mixed tetramers also optimized to distorted tetrahedral structures (**8**, **16** and **9**, **17**). For the lithium halide mixed aggregates, the unsymmetrically mixed tetramer **8** was favored over **9**. The analogous lithium methoxide **16** optimized to a weakly bound complex of the mixed dimer **11** and $(LiOMe)_2$. Of all the lithium methoxide mixed tetramers with $LiCH_2X$, structure **17** was the most energetically favorable. As with the mixed dimer and mixed trimers, the higher temperature disfavored the formation of mixed tetramers. Comparison of the data in Tables 3 and 4 indicates that several lithium halide mixed trimers and tetramers will be present in the gas phase, while the lithium methoxide mixed aggregates will exist almost exclusively as the mixed tetramers **14** and **17**.

Solvation is expected to have a significant effect on the formation of mixed aggregates due to both dipole and steric effects. For the lithium carbenoid (**1**) and lithium halide (**2**) dimers, and for the mixed dimer (**3** or **11**), a question arose as to the number of solvent ligands associated with each lithium atom. Therefore, calculations were performed on the disolvated and tetrasolvated homo- and mixed dimers (Eqs. 20–22), and the results are shown in Table 5.

$$(LiCH_2X)_2\cdot 2THF\ (\mathbf{1}) + 2THF \rightarrow (LiCH_2X)_2\cdot 4THF \quad (20)$$

$$(LiX)_2\cdot 2THF\ (\mathbf{2}) \rightarrow (LiX)_2\cdot 4THF \quad (21)$$

$$(LiCH_2X)(LiX)\cdot 2THF\ (\mathbf{3}\text{ or }\mathbf{11}) + 2THF \rightarrow (LiCH_2X)(LiX)\cdot 4THF \quad (22)$$

The solvation state of the homo- and mixed dimers shows significant temperature dependence, with higher temperatures favoring the disolvated form. Because of the extreme instability of haloalkyllithium carbenoids, reactions are normally performed in a dry ice bath (about 195–200 K) or at even lower temperatures. At 200 K a 1 M solution of the carbenoid would contain the disolvated and tetrasolvated $LiCH_2Cl$ dimers in nearly equal concentrations, and the bromo analog is predominantly the tetrasolvate. The LiX (**2**) and mixed dimer (**3**) are all tetrasolvated at that temperature, and at lower temperatures sometimes required, the $LiCH_2Cl$ dimer will also exist mostly as the tetrasolvate. Therefore, tetrasolvated (**1**), (**2**), and (**3**) were used in the subsequent calculations. The situation is different for the $LiCH_2X$–LiOMe mixed dimers, which the data in Table 5 show to be mostly disolvated by THF, and the disolvated form was used in subsequent calculations.

The formation of THF solvated lithium halide mixed aggregates are described by Eqs. 23–28, and the corresponding lithium methoxide mixed aggregates by Eqs. 29–34. The

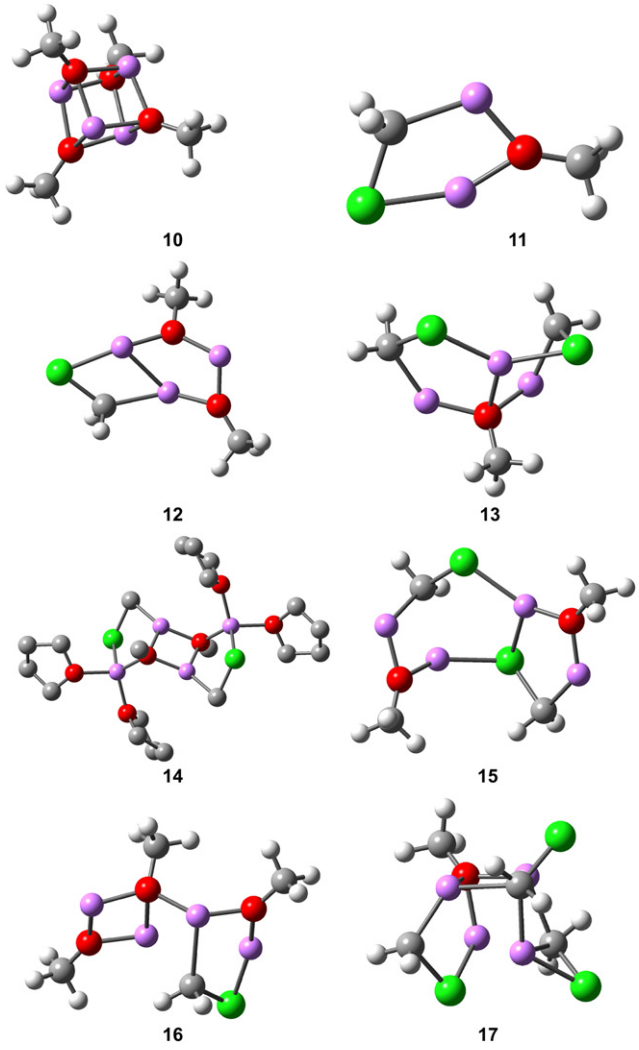

Figure 2. Optimized geometries of lithium carbenoid mixed aggregates with lithium methoxide **10**–**17**.

optimized geometries of the solvated chloromethyllithium–lithium chloride aggregates are shown in Figure 3, and those of the chloromethyllithium–lithium methoxide mixed aggregates in Figure 4.

$$1/2(LiCH_2X)_2\cdot 4THF\ (\mathbf{1}) + 1/2(LiX)_2\cdot 4THF\ (\mathbf{2}) \rightarrow (LiCH_2X)(LiX)\cdot 4THF\ (\mathbf{3}) \quad (23)$$

$$1/2(LiCH_2X)_2\cdot 4THF + (LiX)_2\cdot 4THF \rightarrow (LiCH_2X)(LiX)_2\cdot 3THF\ (\mathbf{4}) + 3THF \quad (24)$$

Table 3. Gas phase free energies of $LiCH_2X$ mixed dimer and mixed trimer formation (kcal/mol per Li) at 200 K (298.15 K)

Mixed aggregates	Temp (K)	Dimer (**3** or **11**)	Trimer (**4** or **12**)	Trimer (**5** or **13**)
$LiCH_2Cl$ LiCl	200	0.164	−3.31	−3.23
$LiCH_2Cl$ LiCl	298.15	0.0650	−2.90	−2.76
$LiCH_2Cl$ LiOMe	200	3.76	2.22	0.556
$LiCH_2Cl$ LiOMe	298.15	3.16	2.12	0.833
$LiCH_2Br$ LiBr	200	0.160	−2.82	−2.60
$LiCH_2Br$ LiBr	298.15	0.0631	−2.43	−2.05
$LiCH_2Br$ LiOMe	200	3.79	2.40	1.43
$LiCH_2Br$ LiOMe	298.15	3.24	2.33	1.78

Table 4. Gas phase free energies of $LiCH_2X$ mixed tetramer formation (kcal/mol per Li) at 200 K (298.15 K)

Mixed aggregates	Temp (K)	Ladder (**6** or **14**)	Tetrahedral or bent (**7** or **15**)	Tetramer (**8** or **16**)	Tetramer (**9** or **17**)
$LiCH_2Cl$ LiCl	200	−5.20	−4.58	−6.57	−2.36
$LiCH_2Cl$ LiCl	298.15	−4.52	−3.52	−5.54	−1.22
$LiCH_2Cl$ LiOMe	200	−1.18	2.95	3.32	−1.93
$LiCH_2Cl$ LiOMe	298.15	−0.747	3.47	3.52	−0.977
$LiCH_2Br$ LiBr	200	−3.69	−2.81	−5.03	−1.13
$LiCH_2Br$ LiBr	298.15	−2.95	−1.72	−4.01	0.00533
$LiCH_2Br$ LiOMe	200	−0.860	3.92	3.60	−1.43
$LiCH_2Br$ LiOMe	298.15	−0.390	4.45	3.82	−0.455

$$(LiCH_2X)_2\cdot 4THF + 1/2(LiX)_2\cdot 4THF \rightarrow (LiCH_2X)_2(LiX)\cdot 3THF\ (\mathbf{5}) + 3THF \quad (25)$$

$$(LiCH_2X)_2\cdot 4THF + (LiX)_2\cdot 4THF \rightarrow (LiCH_2X)_2(LiX)_2\cdot 4THF + 4THF\ (\mathbf{6}\text{ and }\mathbf{7}) \quad (26)$$

$$1/2(LiCH_2X)_2\cdot 4THF + 3/2(LiX)_2\cdot 4THF \rightarrow (LiCH_2X)(LiX)_3\cdot 4THF\ (\mathbf{8}) + 4THF \quad (27)$$

$$3/2(LiCH_2X)_2\cdot 4THF + 1/2(LiX)_2\cdot 4THF \rightarrow (LiCH_2X)_3(LiX)\cdot 4THF\ (\mathbf{9}) + 4THF \quad (28)$$

$$1/2(LiCH_2X)_2\cdot 4THF + 1/4(LiOCH_3)_4\cdot 4THF \rightarrow (LiCH_2X)(LiOCH_3)\cdot 2THF + THF \quad (29)$$

$$1/2(LiCH_2X)_2\cdot 4THF + 1/2(LiOCH_3)_4\cdot 4THF \rightarrow (LiCH_2X)(LiOCH_3)_2\cdot 3THF + THF \quad (30)$$

$$(LiCH_2X)_2\cdot 4THF + 1/4(LiOCH_3)_4\cdot 4THF \rightarrow (LiCH_2X)_2(LiOCH_3)\cdot 3THF + 2THF \quad (31)$$

$$(LiCH_2X)_2\cdot 4THF + 1/2(LiX)_4\cdot 4THF \rightarrow (LiCH_2X)_2(LiX)_2\cdot 4THF + 2THF\ (\mathbf{14}\text{ and }\mathbf{15}) \quad (32)$$

$$1/2(LiCH_2X)_2\cdot 4THF + 3/4(LiOCH_3)_4\cdot 4THF \rightarrow (LiCH_2X)(LiOCH_3)_3\cdot 4THF + THF \quad (33)$$

$$3/2(LiCH_2X)_2\cdot 4THF + 1/4(LiOCH_3)_4\cdot 4THF \rightarrow (LiCH_2X)_3(LiOCH_3)\cdot 4THF + 3THF \quad (34)$$

Table 5. Calculated free energies of tetrasolvated dimer formation (Eqs. 20–22, kcal/mol per Li) at 200 K (298.15 K)

Mixed aggregates	Temp (K)	$(LiCH_2X)_2$ (**1**)	$(LiX)_2$ (**2**)	Mixed dimer (**3**)
$LiCH_2Cl$ LiCl	200	0.0984	−9.31	−6.89
$LiCH_2Cl$ LiCl	298.15	5.93	−3.02	−0.825
$LiCH_2Cl$ LiOMe	200	0.0984	N/A	0.690
$LiCH_2Cl$ LiOMe	298.15	5.93	N/A	7.56
$LiCH_2Br$ LiBr	200	−1.55	−15.7	−9.96
$LiCH_2Br$ LiBr	298.15	3.24	−10.1	−3.93
$LiCH_2Br$ LiOMe	200	−1.55	N/A	1.10
$LiCH_2Br$ LiOMe	298.15	3.24	N/A	8.15

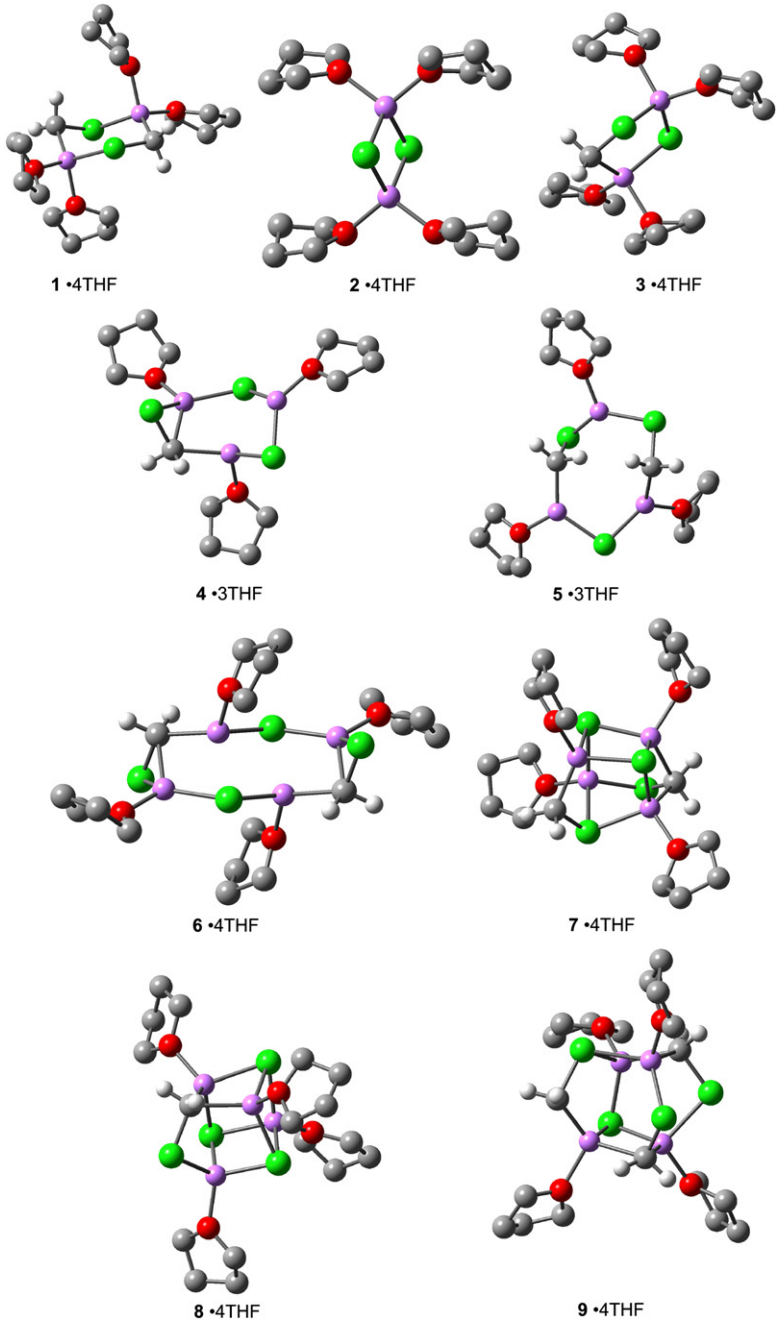

Figure 3. Optimized geometries of THF solvated chloromethyllithium, LiCl, and mixed aggregates **1**–**9**.

Comparison of the data in Tables 3 and 6 shows quite different behavior for the lithium halide and lithium methoxide mixed aggregates. With the lithium halide mixed aggregates, THF solvation has only a small effect on the free energy of mixed dimer formation. At 200 K, the equilibrium constant for LiCl mixed dimer formation will be close to unity, and increase slightly with increasing temperature. The significance of this result is that the mixed dimer cannot be ignored when elucidating reaction mechanisms of chloroalkyllithium carbenoids under conditions where significant amounts of LiCl are present, e.g., late in the reaction. Intentional addition of LiCl to the reaction mixture will also favor formation of the mixed dimer. Formation of the mixed trimers (**4**)·3THF and (**5**)·3THF is energetically unfavorable with respect to the mixed dimer, and showed a similar temperature dependence. Compared to lithium halides, lithium methoxide mixed aggregate formation has a larger temperature dependence, with mixed dimer **11** being favored at room temperature, together with a small amount of mixed trimer **12**. At lower temperatures there is little tendency for lithium methoxide to form mixed dimers or trimers.

Table 7 shows the calculated free energy of formation of the symmetric (**6**, **14** and **7**, **15**) and unsymmetric (**8**, **16** and **9**, **17**) mixed tetramers. In general, mixed tetramer formation with lithium halides is energetically unfavorable at 200 K, but in the case of the lithium chlorocarbenoids, some mixed tetramers may be formed at higher temperatures. The most

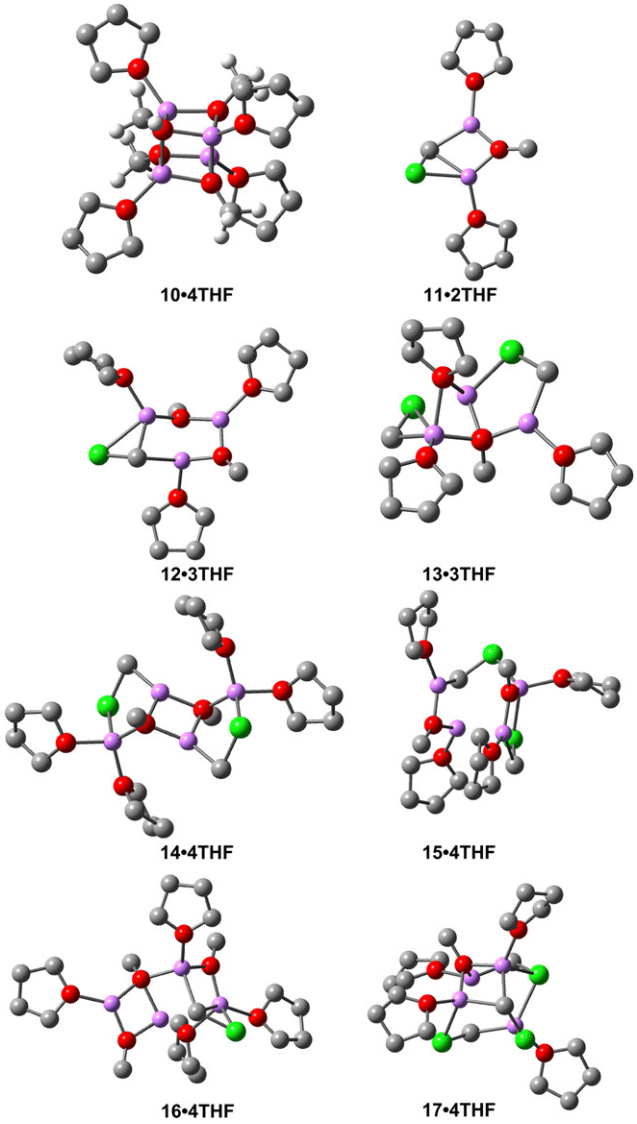

Figure 4. Optimized geometries of THF solvated lithium carbenoid mixed aggregates with lithium methoxide **10**–**17**.

favorable lithium halide mixed tetramer is the $(LiCH_2Cl)$-$(LiCl)_3$ (**8**), which may be present in significant amounts if the reaction mixture contains an excess of lithium chloride. The most favorable solvated $LiCH_2Cl$–lithium methoxide mixed tetramer was **14**, which is favored over the mixed dimers and trimers even at 200 K, and is the only lithium methoxide mixed aggregate that will be formed in appreciable amounts at that temperature.

Table 6. Calculated free energies of THF solvated $LiCH_2X$ mixed dimer and mixed trimer formation (kcal/mol per Li) at 200 K (298.15 K)

Mixed aggregates	Temp (K)	(**3** or **11**)·*n*THF	(**4** or **12**)·3THF	(**5** or **13**)·3THF
$LiCH_2Cl$ LiCl	200	0.0427	3.15	5.66
$LiCH_2Cl$ LiCl	298.15	0.0157	0.790	3.51
$LiCH_2Cl$ LiOMe	200	1.05	1.06	2.07
$LiCH_2Cl$ LiOMe	298.15	−1.17	−0.113	0.590
$LiCH_2Br$ LiBr	200	0.453	5.71	5.61
$LiCH_2Br$ LiBr	298.15	0.778	3.56	3.58
$LiCH_2Br$ LiOMe	200	1.20	0.837	3.25
$LiCH_2Br$ LiOMe	298.15	−0.900	−0.305	2.01

Table 7. Calculated free energies of THF solvated $LiCH_2X$ mixed tetramer formation (kcal/mol per Li) at 200 K (298.15 K)

Mixed Aggregates	Temp (K)	(**6** or **14**)·4THF	(**7** or **15**)·4THF	(**8** or **16**)·4THF	(**9** or **17**)·4THF
$LiCH_2Cl$ LiCl	200	2.68	1.57	0.787	2.29
$LiCH_2Cl$ LiCl	298.15	1.06	−0.351	−1.209	0.464
$LiCH_2Cl$ LiOMe	200	−0.340	2.80	2.87	1.00
$LiCH_2Cl$ LiOMe	298.15	−1.73	1.76	2.36	−0.377
$LiCH_2Br$ LiBr	200	5.27	5.25	4.48	5.27
$LiCH_2Br$ LiBr	298.15	3.69	3.59	2.48	3.56
$LiCH_2Br$ LiOMe	200	1.11	4.18	3.02	2.47
$LiCH_2Br$ LiOMe	298.15	0.0229	3.25	2.57	1.25

Halomethyllithium carbenoids could potentially undergo cyclopropanation reactions via a monomer, homo-dimer, or mixed dimer. To test the hypothesis concerning changes in lithium carbenoid reaction pathways caused by mixed aggregates, the gas phase activation barrier for the cyclopropanation reaction of chloromethyllithium with ethylene was calculated. Although DFT methods generally generate good geometries and energies for ground state species, they are less reliable for transition structure and activation barrier calculations.[23] The activation free energies were calculated at the Hartree–Fock, B3LYP, and MP2 levels, each with the 6-31+G(d) basis set, and the results are shown in Table 8. At the MP2 level, the calculated activation barrier for the mixed dimer (**3**) was lower than that of the chloromethyllithium homo-dimer by 1.0 kcal/mol and lower than that of the monomer by 0.5 kcal/mol. A comprehensive study on the role of mixed aggregates in carbenoid reactions is beyond the scope of this paper and will be the subject of a study in the near future. However, these preliminary calculations show that mixed aggregate formation in these reactions cannot be ignored under conditions where lithium halides are present in significant amounts, such as near the end of the reaction. Even with such a relatively small change in activation energies, the mechanism is subjected to change as new potentially reactive species are formed. After a few half lives the reaction mechanism may change at least once and perhaps twice if significant amounts of tetramer are present after several half lives.

Table 8. Calculated gas phase activation free energies of cyclopropanation reactions of $LiCH_2Cl$ aggregates with ethylene (kcal/mol)

Aggregate	Hartree–Fock	B3LYP	MP2
Monomer	14.2	14.2	17.1
Dimer (**1**)	11.1	15.4	17.6
Mixed dimer (**3**)	9.45	14.2	16.6

4. Conclusions

Lithium halomethyllithium carbenoids can form mixed aggregates with lithium halides. In the gas phase, mixed trimers and tetramers are formed preferentially over mixed dimers. THF solvation disfavors the formation of the mixed trimers and tetramers, but has only a small effect on the free energy of mixed dimer formation. At temperatures below 200 K, chloromethyllithium, and to a lesser extent, bromomethyllithium mixed dimers will coexist with the free carbenoids. Mixed aggregate formation can affect the activation

barriers of carbenoid reactions and may cause a change in the mechanism during the course of a reaction.

In the gas phase, chloro- and bromomethyllithium can form two different mixed tetramers with lithium methoxide. Formation of mixed dimers and trimers is energetically unfavorable. Solvation with THF reduces the tendency of these carbenoids to form mixed aggregates, although there appears to be a modest tendency toward mixed tetramer formation.

The major significance of this work is that the mixed aggregate formation can affect the activation barriers of carbenoid reactions and may cause a change in the mechanism during the course of the reaction. Similar mixed aggregates have been exploited to alter the reactivity and stereoselectivity of other organolithium reagents. The mixed aggregates described in this paper have potential for use in synthetic reactions of lithium carbenoids.

Acknowledgements

This research used resources of the National Energy Research Scientific Computing Center, which is supported by the Office of Science of the U.S. Department of Energy under Contract No. DE-AC03-76SF00098. This work was also supported by DOE Grant # DE-FG02-02ER25544, and by NSF grant #INT-0454045. Thanks to B. Ramachandran at Louisiana Tech for his lecture notes on which the 'Derivation of standard state equations' section of the supplementary materials is based.

Supplementary data

Tables of optimized geometries and energies of all reactants, and a derivation of the standard state equations. Supplementary data associated with this article can be found in the online version, at doi:10.1016/j.tet.2006.08.104.

References and notes

1. Seebach, D.; Siegel, H.; Mullen, K.; Hiltbrunner, K. *Angew. Chem., Int. Ed. Engl.* **1979**, *18*, 784.
2. Seebach, D.; Siegel, H.; Gabriel, J.; Hassig, R. *Helv. Chim. Acta* **1980**, *63*, 2046.
3. Nakamura, M.; Hirai, A.; Nakamura, E. *J. Am. Chem. Soc.* **2003**, *125*, 2341.
4. Wang, D.; Phillips, D. K. *Organometallics* **2002**, *21*, 5901.
5. Hermann, H.; Lohrenz, J. C. W.; Kuhn, A.; Boche, G. *Tetrahedron* **2000**, *56*, 4109.
6. Pratt, L. M.; Ramachandran, B.; Xidos, J. D.; Cramer, C. J.; Truhlar, D. G. *J. Org. Chem.* **2002**, *67*, 7607.
7. Corey, E. J.; Gross, A. W. *Tetrahedron Lett.* **1984**, *25*, 495.
8. Hall, P. L.; Gilchrist, J. H.; Collum, D. B. *J. Am. Chem. Soc.* **1991**, *113*, 9571.
9. Hall, P. L.; Gilchrist, J. H.; Harrison, A. T.; Fuller, D. J.; Collum, D. B. *J. Am. Chem. Soc.* **1991**, *113*, 9575.
10. Pratt, L. M.; Newman, A.; St. Cyr, J.; Johnson, H.; Miles, B.; Lattier, A.; Austin, E.; Henderson, S.; Hershey, B.; Lin, M.; Balamraju, Y.; Sammonds, L.; Cheramie, J.; Karnes, J.; Hymel, E.; Woodford, B.; Carter, C. *J. Org. Chem.* **2003**, *68*, 6387.
11. Balamraju, Y.; Sharp, C. D.; Gammill, W.; Manuel, N.; Pratt, L. M. *Tetrahedron* **1998**, *54*, 7357.
12. Pratt, L. M. *Bull. Chem. Soc. Jpn.* **2005**, *78*, 890.
13. Pratt, L. M.; Le, L. T.; Truong, T. N. *J. Org. Chem.* **2005**, *70*, 8298.
14. Frisch, M. J.; Trucks, G. W.; Schlegel, H. B.; Scuseria, G. E.; Robb, M. A.; Cheeseman, J. R.; Montgomery, J. A., Jr.; Vreven, T.; Kudin, K. N.; Burant, J. C.; Millam, J. M.; Iyengar, S. S.; Tomasi, J.; Barone, V.; Mennucci, B.; Cossi, M.; Scalmani, G.; Rega, N.; Petersson, G. A.; Nakatsuji, H.; Hada, M.; Ehara, M.; Toyota, K.; Fukuda, R.; Hasegawa, J.; Ishida, M.; Nakajima, T.; Honda, Y.; Kitao, O.; Nakai, H.; Klene, M.; Li, X.; Knox, J. E.; Hratchian, H. P.; Cross, J. B.; Adamo, C.; Jaramillo, J.; Gomperts, R.; Stratmann, R. E.; Yazyev, O.; Austin, A. J.; Cammi, R.; Pomelli, C.; Ochterski, J. W.; Ayala, P. Y.; Morokuma, K.; Voth, G. A.; Salvador, P.; Dannenberg, J. J.; Zakrzewski, V. G.; Dapprich, S.; Daniels, A. D.; Strain, M. C.; Farkas, O.; Malick, D. K.; Rabuck, A. D.; Raghavachari, K.; Foresman, J. B.; Ortiz, J. V.; Cui, Q.; Baboul, A. G.; Clifford, S.; Cioslowski, J.; Stefanov, B. B.; Liu, G.; Liashenko, A.; Piskortz, P.; Komaromi, I.; Martin, R. L.; Fox, D. J.; Keith, T.; Al-Laham, M. A.; Peng, C. Y.; Nanayakkara, A.; Challacombe, M.; Gill, P. M. W.; Johnson, B.; Chem, W.; Wong, M. W.; Gonzalez, C.; Pople, J. A. *Gaussian 03, Revision A.1*; Gaussian: Pittsburgh, PA, 2003.
15. Becke, A. D. *J. Chem. Phys.* **1993**, *98*, 5648.
16. Stephens, P. J.; Devlin, F. J.; Chabalowski, G. C.; Frisch, M. J. *J. Phys. Chem.* **1994**, *98*, 11623.
17. Thompson, J. D.; Winget, P.; Truhlar, D. G. *Phys. Chem. Commun.* **2001**, *16*, 1.
18. Lynch, B. J.; Zhao, Y.; Truhlar, D. G. *J. Phys. Chem.* **2003**, *107*, 1384.
19. Clark, T.; Chandresekhar, J.; Schleyer, P. v. R. *J. Comput. Chem.* **1983**, *4*, 294.
20. Thompson, J. D.; Cramer, C. J.; Truhlar, D. G. *J. Chem. Phys.* **2003**, *119*, 1661.
21. Govender, U. P.; Letcher, T. M.; Garg, S. K.; Ahluwalia, J. C. *J. Chem. Eng. Data* **1996**, *41*, 147.
22. Wong, M. K.; Popov, A. I. *J. Inorg. Nucl. Chem.* **1972**, *34*, 3615.
23. Pratt, L. M.; Nguyen, N. V.; Ramachandran, B. *J. Org. Chem.* **2005**, *70*, 4.